

Article

# Linear Stability of Filtration Flow of a Gas and Two Immiscible Liquids with Interfaces

Vladimir Shargatov \* , George Tsypkin  and Polina Kozhurina 

Ishlinsky Institute for Problems in Mechanics of the Russian Academy of Sciences, 119526 Moscow, Russia; tsypkin@ipmnet.ru (G.T.)

\* Correspondence: shargatov@mail.ru

**Abstract:** The stability of the vertical flow that occurs when gas displaces oil from a reservoir is investigated. It is assumed that the oil and gas areas are separated by a layer saturated with water. This method of oil displacement, called water-alternating-gas injection, improves the oil recovery process. We consider the linear stability of two boundaries that are flat at the initial moment, separating, respectively, the areas of gas and water, as well as water and oil. The instability of the interfaces can result in gas and water fingers penetrating into the oil-saturated area and causing residual oil. Two cases of perturbation evolution are considered. In the first case, only the gas–water interface is perturbed at the initial moment, and in the second case, small perturbations of the same amplitude are present on both surfaces. It is shown that the interaction of perturbations at interfaces depends on the thickness of the water-saturated layer, perturbation wavelength, oil viscosity, pressure gradient and formation thickness. Calculations show that perturbations at the oil–water boundary grow much slower than perturbations at the gas–water boundary. It was found that, with other parameters fixed, there is a critical (or threshold) value of the thickness of the water-saturated layer, above which the development of perturbations at the gas–water boundary does not affect the development of perturbations at the water–oil boundary.

**Keywords:** porous media; water–oil interface; gas–water interface; instability; fingering; water-alternating-gas injection; displacement

**MSC:** 35Q35; 35B35



**Citation:** Shargatov, V.; Tsypkin, G.; Kozhurina, P. Linear Stability of Filtration Flow of a Gas and Two Immiscible Liquids with Interfaces. *Mathematics* **2023**, *11*, 4476. <https://doi.org/10.3390/math11214476>

Academic Editor: Nikolai A. Kudryashov

Received: 4 October 2023  
Revised: 24 October 2023  
Accepted: 26 October 2023  
Published: 28 October 2023



**Copyright:** © 2023 by the authors. Licensee MDPI, Basel, Switzerland. This article is an open access article distributed under the terms and conditions of the Creative Commons Attribution (CC BY) license (<https://creativecommons.org/licenses/by/4.0/>).

## 1. Introduction

Oil fields with a gas cap comprise a significant proportion of gas and oil fields [1]. Oil production from such deposits has specific characteristics and differs from the development of pure oil deposits [2]. A decrease in pressure in the oil-saturated region causes movement of the gas–oil contact surface. It may be unstable and lead to gas breakdown in the production well. As a result, residual oil is formed in the reservoir [3]. In addition, the instability and breakdown of gas–oil and water–oil surfaces can lead to discontinuity and fragmentation of the oil flow, which also causes the formation of residual oil in the field [4].

Displacing oil from the reservoir by gas is an effective method for increasing oil recovery [5]. The process is more efficient if water displacement is injected first, then gas. In this case, gas and oil are separated by a layer of water, and both the water–gas and water–oil boundaries are unstable. Carbon dioxide is injected into depleted oil reservoirs for storage purposes to reduce climatic impacts and improve oil recovery [6]. In this process, gas is often injected into a porous medium filled with water and oil. Thus, studying the evolution of the water–gas and water–oil interfaces and the mutual influence of these processes is an important task.

Recently, analytical and numerical studies have been carried out on the instability of the interface boundary during filtration in soils and rocks [7]. It was found that in many

cases, important for applications, the transition to instability occurs for all values of the wave number simultaneously or at infinitely large wave numbers [7]. The fastest-growing mode of the unsteady flow is the mode corresponding to an infinitesimal linear size. Finding the parameters of the fastest-growing perturbation is of interest for determining the characteristic scale of the resulting finger-like structures, the decay of which leads to volumes of liquid. In the classical work [8], the problem of the instability of the displacement of a more viscous liquid by a less viscous one was considered. The transition to instability occurred simultaneously at all wave numbers, which did not make it possible to establish the characteristic size of the most unstable perturbation. In [9], the stability of the gas–oil interface in a gas cap under a pressure drop in the oil-saturated region was studied. A criterion for surface stability was found, showing that when the parameters change, the transition to the unstable regime is also realized simultaneously at all wave numbers.

However, it was shown in [10] that anomalous short-wave instability does not occur if the Brinkman equation is used instead of Darcy’s law. Using the normal mode method, it was found that the growth rate of small perturbations of the liquid–gas surface tends to zero with increasing wave number. An extensive review of experimental studies of three-phase relative permeability is presented in [11]. The results of a pore-scale experimental survey of a two-phase oil/brine flow through a miniature, water-wet fractured sandstone core sample were presented in [12].

There are several approaches to studying the process of liquid displacement by gas. In the piston model (continuum single-phase model) of displacement, it is assumed that there is either gas, water, or oil at each point of the medium. In this case, it is assumed that there is a boundary between different liquids, as well as between a liquid and a gas, which, in a large-scale approximation, represents a moving surface. This model was used to study the main features of the development of instability in many works (see, for example, Ref. [13] and the review in [14]). The problem of the displacement of one incompressible fluid by another in an inhomogeneous layered porous medium was also studied in [15]. In this case, it was assumed that the injected fluid completely displaces the previously filling fluid, and there is a moving interface between them.

Using the three-phase continuum approach, three phases (water, oil and gas) are expected to coexist at every point in the porous medium when viewed from a macroscopic point of view (see, for example, Refs. [16,17] and a detailed review in [18]). General analytical solutions for a three-phase immiscible flow in a one-dimensional porous medium with concave relative permeability curves are presented in [19].

Along with the continuum approximation, network models are used to study oil displacement processes [20]. The network model allows us to take into account processes occurring at the micro level. Thus, it is assumed that water, oil and gas flow in close but different channels or are separated within each. For example, in [21], the process of the displacement of oil from the reservoir by gas is considered. It is assumed that gas, water and oil formally exist at every point in the medium at the macro level, but at the micro level, they are located in separate, closely spaced pores. In [22], drainage displacements in a three-phase flow under strongly wetting conditions are described by the pore-scale network model. In [23], the oil and gas outflow process is also described using a three-dimensional network model. Agreement between the calculated and experimental data was obtained.

It is important to note that there is a problem of sediment formation when water is injected into the reservoir. Asphaltene possess the ability to accumulate at the interface of oil and water, leading to the formation of stable emulsions. An experimental investigation of this phenomena is presented in [24]. Molecular dynamics simulations are developed in [24]. The effect of ions in water on asphaltene aggregation was studied in [25]. The influence of water cut on the effectiveness of an asphaltene inhibitor was investigated in [26].

An interesting and promising approach is a combined multiphase lattice Boltzmann color-gradient model for simulating the flow of immiscible two- and three-phase liquids (see, for example, Ref. [6]). In [9], a single-phase continuum model was used to study the development of gas–liquid interface instability in a porous medium. It is shown that at the

initial stage of the development of a perturbation, the results obtained by the normal mode method for linearized equations of a single-phase continuum model are consistent with the solution of the nonlinear problem. At the same time, using the network model makes it possible to obtain qualitative results that are consistent with the single-phase continuum model results.

In this paper, a single-phase continuum model is used to describe the evolution of gas–water and water–oil interface perturbations. The main novelty of this work is that analytical solutions have been obtained that describe the main patterns of the mutual influence of the development of disturbances at the water–gas and water–oil boundaries.

The paper is organized as follows: Section 2 contains the formulation of the problem within the continuum model using Darcy’s law. The specific boundary conditions are given. Next, the governing equations and the boundary conditions are made dimensionless. In Section 3, a vertical flow solution is obtained for the stability study. The water–gas and water–oil interfaces are initially assumed to be flat. Time-dependent pressure and velocity profiles are obtained. In Section 4, a linear stability analysis of the basic solution is presented. The governing equations and boundary conditions are linearized about the basic solution. According to the classical procedure, the normal mode method is used to study the behaviour of the perturbed interfaces. The problem of the evolution of infinitesimal perturbations of gas–water and oil–water surfaces is solved in a linear approximation, taking into account their mutual influence. Section 5 contains a discussion of the results obtained. In the conclusion, the main results of the work are summarized. Appendix A contains a derivation of approximate formulas for large and small values of the dimensionless wave number.

**2. Formulation of the Problem**

We consider water and oil filtration in a horizontal layer of porous medium (Figure 1). Region 0 is filled with gas. The pressure in this region is assumed to be constant and equal to  $P_a^*$ . Region 1 is filled with water with parameters  $\mu_1^*$  and  $\rho_1^*$  of viscosity and density, respectively. There exists a water–gas interface that separates the water from the gas. A continuous pressure at this interface is prescribed. At the lower boundary, region 1 is in contact with layer 2, which is oil-saturated with the corresponding viscosity and density parameters  $\mu_2^*$  and  $\rho_2^*$ . The  $z^*$ -coordinates of the gas–water and water–oil interfaces are described by the functions  $S_1^*(x^*, t^*)$  and  $S_2^*(x^*, t^*)$ , respectively. Regions 0, 1 and 2 are located inside a relatively low-permeability porous medium layer. Region 3 contains a highly permeable layer modelling a horizontal well or fracture with constant pressure,  $P_L^*$ .

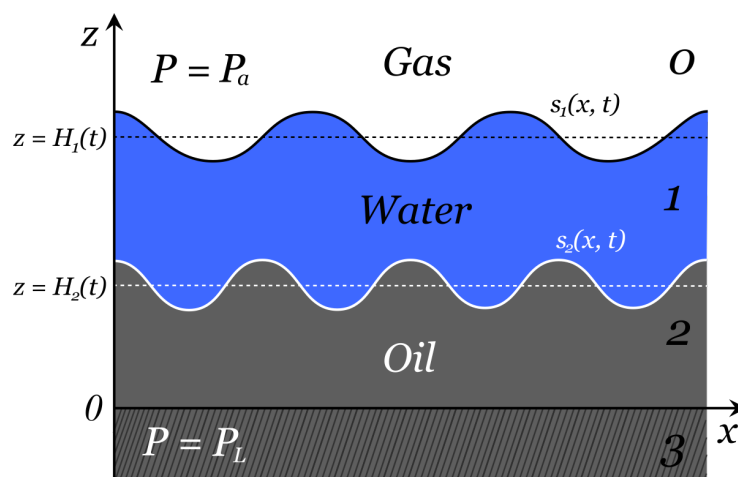


**Figure 1.** Scheme of the considered porous medium layer.

The fluids are assumed to be incompressible, and the filtration flow is described by Darcy’s equation [27]:

$$\operatorname{div} \vec{v}_i^* = 0, \quad \vec{v}_i^* = (v_{ix}^*, v_{iz}^*), \tag{1a}$$

$$0 = -\nabla(P_i^* + \rho_i^* g^* z^*) - \frac{\mu_i^*}{k^*} \vec{v}_i^*, \quad i = 1, 2, \tag{1b}$$

where  $\vec{v}_i^*$  is the filtration velocity,  $P_i^*$  is the pressure,  $\rho_i^*$  is the density,  $g^*$  is the acceleration due to gravity,  $\mu_i^*$  is the viscosity,  $k^*$  is the permeability and the subscripts 1 and 2 correspond to the water and oil regions, respectively.

According to [27], we solve these equations subject to the boundary conditions of constant pressure on the gas–water interface and on the lower boundary of region 2. In addition, the flow fields in layers 1 and 2 (see Figure 1) are coupled by the requirements of pressure continuity across the water–oil interface and no flow through this interface. The pressure continuity condition neglects the effect of capillary pressure because the general question of the stability or instability of the interfaces is independent of the inclusion of this phenomenon [27].

The boundary condition at the gas–water interface ( $z^* = S_1^*(x^*, t^*)$ ) is

$$P_1^*(x^*, S_1^*(x^*, t^*), t^*) = P_a^*. \tag{2}$$

The pressure is equal to  $P_L^*$  at the lower boundary of the region saturated with oil. The corresponding boundary condition can be written as

$$P_2^*(x^*, 0, t^*) = P_L^*. \tag{3}$$

If the pressure and the normal component of velocity at the water–oil interface ( $z^* = S_2^*(x^*, t^*)$ ) are continuous, then we obtain

$$P_1^*(x^*, S_2^*(x^*, t^*), t^*) = P_2^*(x^*, S_2^*(x^*, t^*), t^*), \tag{4}$$

$$(\vec{v}_1^*(x^*, S_2^*(x^*, t^*), t^*), \vec{N}^*(x^*, S_2^*(x^*, t^*), t^*)) = (\vec{v}_2^*(x^*, S_2^*(x^*, t^*), t^*), \vec{N}^*(x^*, S_2^*(x^*, t^*), t^*)), \tag{5}$$

where

$$\vec{N}^*(x^*, S_i^*(x^*, t^*), t^*) = \left\{ -\frac{\frac{\partial S_i^*(x^*, t^*)}{\partial x^*}}{\sqrt{1 + \left(\frac{\partial S_i^*(x^*, t^*)}{\partial x^*}\right)^2}}, \frac{1}{\sqrt{1 + \left(\frac{\partial S_i^*(x^*, t^*)}{\partial x^*}\right)^2}} \right\}. \tag{6}$$

The evolution of the interfaces between gas and water and water and oil is described by the equations

$$\frac{\partial}{\partial t^*} S_1^*(x^*, t^*) = v_{1z}^* - v_{1x}^* \frac{\partial}{\partial x^*} S_1^*(x^*, t^*), \tag{7}$$

$$\frac{\partial}{\partial t^*} S_2^*(x^*, t^*) = v_{2z}^* - v_{2x}^* \frac{\partial}{\partial x^*} S_2^*(x^*, t^*). \tag{8}$$

Equations (7) and (8) will be used in the form

$$\frac{\partial}{\partial t^*} S_1^*(x^*, t^*) = (\vec{v}_1^*(x^*, S_1^*(x^*, t^*), t^*), \vec{n}^*(x^*, S_1^*(x^*, t^*), t^*)), \tag{9}$$

$$\frac{\partial}{\partial t^*} S_2^*(x^*, t^*) = (\vec{v}_2^*(x^*, S_2^*(x^*, t^*), t^*), \vec{n}^*(x^*, S_2^*(x^*, t^*), t^*)), \tag{10}$$

where

$$\vec{n}^*(x^*, S_i^*(x^*, t^*), t^*) = \left\{ -\frac{\partial S_i^*(x^*, t^*)}{\partial x^*}, 1 \right\}. \tag{11}$$

The governing equations and the boundary conditions are made dimensionless using the following reference parameters

$$x = \frac{x^*}{H_0^*}, z = \frac{z^*}{H_0^*}, \vec{v}_i = \frac{\vec{v}_i^*}{V_0^*}, t = \frac{t^* V_0^*}{H_0^*}, k_i = \frac{k^* P_0^*}{\mu_i^* V_0^* H_0^*}, g = g^* \frac{V_0^{*2}}{H_0^*}, \tag{12}$$

$$P_i = \frac{P_i^*}{P_0^*}, \rho_i = \rho_i^* \frac{V_0^{*2}}{P_0^*},$$

where  $P_0^*$  is characteristic pressure,  $H_0^*$  is characteristic size and  $V_0^*$  is characteristic velocity.

The governing equations and the boundary conditions, using the normalised quantities (12), take the form

$$\text{div } \vec{v}_i = 0, \tag{13a}$$

$$0 = -\nabla(P_i + \rho_i g z) - \frac{1}{k_i} \vec{v}_i, \quad i = 1, 2, \tag{13b}$$

$$P_1(x, S_1(x, t), t) = P_a, \tag{14}$$

$$P_2(x, 0, t) = P_L, \tag{15}$$

$$P_1(x, S_2(x, t), t) = P_2(x, S_2(x, t), t), \tag{16}$$

$$(\vec{v}_1(x, S_2(x, t), t), \vec{N}(x, S_2(x, t), t)) = (\vec{v}_2(x, S_2(x, t), t), \vec{N}(x, S_2(x, t), t)), \tag{17}$$

$$\vec{N}(x, S_i(x, t), t) = \left\{ -\frac{\frac{\partial S_i(x, t)}{\partial x}}{\sqrt{1 + \left(\frac{\partial S_i(x, t)}{\partial x}\right)^2}}, \frac{1}{\sqrt{1 + \left(\frac{\partial S_i(x, t)}{\partial x}\right)^2}} \right\}, \tag{18}$$

$$\frac{\partial}{\partial t} S_1(x, t) = (\vec{v}_1(x, S_1(x, t), t), \vec{n}(x, S_1(x, t), t)), \tag{19}$$

$$\frac{\partial}{\partial t} S_2(x, t) = (\vec{v}_1(x, S_2(x, t), t), \vec{n}(x, S_2(x, t), t)), \tag{20}$$

$$\vec{n}(x, S_i(x, t), t) = \left\{ -\frac{\partial S_i(x, t)}{\partial x}, 1 \right\}. \tag{21}$$

### 3. Vertical Flow Solution

Let the boundaries between regions 0 and 1 and regions 1 and 2 be flat and perpendicular to the axis  $z$ . In this case, the solution is independent of the horizontal variable  $x$ , so  $P_1, P_2, v_1$  and  $v_2$  are all functions of  $z$  only, i.e.,  $P_1 = P_{1,b}(z, t), P_2 = P_{2,b}(z, t), \vec{v}_1 = (0, V_{1,b}(z, t)), \vec{v}_2 = (0, V_{2,b}(z, t)), S_1 = H_1(t)$  and  $S_2 = H_2(t)$  (see Figure 1). The subscript  $b$  denotes the basic vertical flow solution of Equations (13a) and (13b) with boundary conditions (14)–(17). The equations governing the basic vertical flow will take the form

$$\frac{\partial V_{1,b}}{\partial z} = 0, \quad \frac{\partial V_{2,b}}{\partial z} = 0, \tag{22}$$

$$0 = -\frac{\partial P_{1,b}}{\partial z} - \rho_1 g - \frac{1}{k_1} V_{1,b}, \quad 0 = -\frac{\partial P_{2,b}}{\partial z} - \rho_2 g - \frac{1}{k_2} V_{2,b}. \tag{23}$$

The solutions of (22) for the velocity distribution subject to the boundary condition in (17) are

$$V_{1,b}(z, t) = \bar{V}(t), \quad V_{2,b}(z, t) = \bar{V}(t). \tag{24}$$

Substituting velocities (24) into (23) yields

$$0 = -\frac{\partial P_{1,b}}{\partial z} - \rho_1 g - \frac{1}{k_1} \bar{V}(t), \quad 0 = -\frac{\partial P_{2,b}}{\partial z} - \rho_2 g - \frac{1}{k_2} \bar{V}(t). \tag{25}$$

The solutions of (25) give the linear pressure profile:

$$P_{1,b} = -(\rho_1 g + \frac{1}{k_1} \bar{V}(t))(z - H_1(t)) + P_a, \tag{26}$$

$$P_{2,b} = -(\rho_2 g + \frac{1}{k_2} \bar{V}(t))z + P_L. \tag{27}$$

Thus, from the boundary condition in (16), we obtain

$$-(\rho_1 g + \frac{1}{k_1} \bar{V}(t))(H_2(t) - H_1(t)) + P_a = -(\rho_2 g + \frac{1}{k_2} \bar{V}(t))H_2(t) + P_L. \tag{28}$$

Hence, the expression follows

$$\bar{V}(t) = -\frac{k_1 k_2 (g(\rho_2 - \rho_1)H_2(t) + g\rho_1 H_1(t) + P_a - P_L)}{(k_1 - k_2)H_2(t) + H_1(t)k_2}. \tag{29}$$

The solutions of (23) for  $P_{1,b}$  and  $P_{2,b}$  subject to the pressure boundary conditions in (14)–(16) are

$$P_{1,b}(z, t) = \frac{(g(k_1\rho_1 - k_2\rho_2)H_1(t) + (g\rho_2 z - P_a)k_2 - k_1(g\rho_1 z - P_a))H_2(t) + k_2(H_1(t)P_L - z(P_L - P_a))}{(k_1 - k_2)H_2(t) + H_1(t)k_2}, \tag{30}$$

$$P_{2,b}(z, t) = \frac{((-g\rho_1 z + P_L)k_1 + k_2(g\rho_2 z - P_L))H_2(t) + (gzk_1\rho_1 - k_2(g\rho_2 z - P_L))H_1(t) - zk_1(P_L - P_a)}{(k_1 - k_2)H_2(t) + H_1(t)k_2}, \tag{31}$$

and the z-coordinates of the interfaces  $H_1(t)$  and  $H_2(t)$  satisfy the equations

$$\begin{cases} \frac{dH_1(t)}{dt} = \bar{V}(t), \\ \frac{dH_2(t)}{dt} = \bar{V}(t). \end{cases} \tag{32}$$

It follows from (32) that

$$H_1(t) - H_2(t) = H_1(0) - H_2(0). \tag{33}$$

We introduce the notation

$$L = H_1(t) - H_2(t), \tag{34}$$

where  $L$  is independent of  $t$ .

The solution of (32) for the function  $t(H_2)$  is

$$t(H_2) = \frac{(-C_a C_c L + C_b) \ln \frac{(H_2 C_a + C_b)}{(H_2(0) C_a + C_b)}}{C_a^2} - \frac{H_2 - H_2(0)}{C_a}, \tag{35}$$

where

$$C_a = \rho_2 g k_2, \tag{36}$$

$$C_b = L g \rho_1 k_2 + \Delta P k_2, \tag{37}$$

$$C_c = \frac{k_2}{k_1}, \tag{38}$$

$$\Delta P = P_a - P_L. \tag{39}$$

We can find the function  $H_2(t)$  from (35). The function  $H_1(t)$  is defined as

$$H_1(t) = H_2(t) + L. \tag{40}$$

At  $g = 0$ , the expression (35) has a simpler form

$$t(H_2)_{g=0} = \frac{(2k_2L + k_1(H_2 + H_2(0)))(H_2(0) - H_2)}{2\Delta P k_1 k_2}. \tag{41}$$

#### 4. Evolution of Infinitesimal Perturbations of Vertical Flow

We now consider the stability of the solution (29)–(31) to infinitesimal perturbations derived in the previous section. An infinitesimal perturbation is applied to the basic flow to examine the stability of the interfaces. The aim is to linearise the governing equations and boundary conditions about the basic solution (29)–(31) and to study the behaviour of the perturbed interfaces. The velocity and pressure fields both in the water and oil regions and the interface positions are expanded in the following manner:

$$S_1(x, t) = H_1(t) + s_1(x, t), \tag{42}$$

$$S_2(x, t) = H_2(t) + s_2(x, t), \tag{43}$$

$$P_1(x, z, t) = P_{1,b}(z, t) + p_1(x, z, t), \tag{44}$$

$$P_2(x, z, t) = P_{2,b}(z, t) + p_2(x, z, t), \tag{45}$$

$$v_{1z}(x, z, t) = \bar{V}(t) + v_1(x, z, t), \tag{46}$$

$$v_{2z}(x, z, t) = \bar{V}(t) + v_2(x, z, t), \tag{47}$$

$$v_{1x}(x, z, t) = u_1(x, z, t), \tag{48}$$

$$v_{2x}(x, z, t) = u_2(x, z, t), \tag{49}$$

where  $s_1(x, t)$ ,  $s_2(x, t)$ ,  $p_1(x, z, t)$ ,  $p_2(x, z, t)$ ,  $u_1(x, z, t)$ ,  $v_1(x, z, t)$ ,  $u_2(x, z, t)$  and  $v_2(x, z, t)$  are small perturbations of the positions of the gas–water and water–oil interfaces, the pressure, and the horizontal and vertical components of the filtration velocity in the regions filled with water and oil, respectively.

Let us obtain the basic equations of the problem in a linearized form. We substitute the expressions (42)–(49) into the system of Equations (13):

$$\frac{\partial(P_{i,b}(z, t) + p_i(x, z, t))}{\partial z} = -\frac{\bar{V}(t) + v_i(x, z, t)}{k_i} - \rho_i g, \tag{50}$$

$$\frac{\partial(P_{i,b}(z, t) + p_i(x, z, t))}{\partial x} = -\frac{u_i(x, z, t)}{k_i}, \tag{51}$$

$$\frac{\partial}{\partial x} u_i(x, z, t) + \frac{\partial}{\partial z} (\bar{V}(t) + v_i(x, z, t)) = 0, \quad i = 1, 2. \tag{52}$$

The boundary conditions are

$$P_{1,b}(H_1(t) + s_1(x, t), t) + p_1(x, H_1(t) + s_1(x, t), t) = P_a, \tag{53}$$

$$P_{2,b}(0, t) + p_2(x, 0, t) = P_L, \tag{54}$$

$$\begin{aligned} &P_{1,b}(H_2(t) + s_2(x, t), t) + p_1(x, H_2(t) + s_2(x, t), t) \\ &= P_{2,b}(H_2(t) + s_2(x, t), t) + p_2(x, H_2(t) + s_2(x, t), t). \end{aligned} \tag{55}$$

The system of equations for perturbations has the form

$$\begin{cases} \frac{\partial p_i(x, z, t)}{\partial z} = -\frac{v_i(x, z, t)}{k_i}, \\ \frac{\partial p_i(x, z, t)}{\partial x} = -\frac{u_i(x, z, t)}{k_i}, \\ \frac{\partial}{\partial x} u_i(x, z, t) + \frac{\partial}{\partial z} v_i(x, z, t) = 0, \end{cases} \tag{56}$$

and the boundary conditions expressed as:

$$s_1(x, t) \frac{\partial}{\partial z} P_{1,b}(z, t)|_{z=H_1(t)} + p_1(x, H_1(t), t) = 0, \tag{57}$$

$$p_2(x, 0, t) = 0, \tag{58}$$

$$\begin{aligned} &s_2(x, t) \frac{\partial}{\partial z} P_{1,b}(z, t)|_{z=H_2(t)} + p_1(x, H_2(t), t) \\ &= s_2(x, t) \frac{\partial}{\partial z} P_{2,b}(z, t)|_{z=H_2(t)} + p_2(x, H_2(t), t), \end{aligned} \tag{59}$$

$$v_1(x, H_2(t), t) = v_2(x, H_2(t), t), \tag{60}$$

$$\frac{\partial}{\partial t} s_1(x, t) = v_1(x, H_1(t), t), \tag{61}$$

$$\frac{\partial}{\partial t} s_2(x, t) = v_1(x, H_2(t), t). \tag{62}$$

We assume that the solutions for  $p_i(x, z, t)$ ,  $u_i(x, z, t)$ ,  $v_i(x, z, t)$  and  $s_i(x, z, t)$  have the form

$$p_i(x, z, t) = \Pi_i(z) f(t) \exp(iKx), \tag{63}$$

$$u_i(x, z, t) = U_i(z) f(t) \exp(iKx), \tag{64}$$

$$v_i(x, z, t) = V_i(z) f(t) \exp(iKx), \tag{65}$$

$$s_1(x, t) = C_5 f(t) \exp(iKx), \tag{66}$$

$$s_2(x, t) = C_6 f(t) \exp(iKx). \tag{67}$$

Substituting (63)–(65) into (56) yields

$$\begin{cases} \frac{\partial \Pi_i(z)}{\partial z} = -\frac{V_i(z)}{k_i}, \\ iK \Pi_i(z) = -\frac{U_i(z)}{k_i}, \\ 0 = iK U_i(z) + \frac{\partial V_i(z)}{\partial z}. \end{cases} \tag{68}$$



The solutions of (68) have the form

$$\begin{cases} \Pi_1(z) = C_3e^{-Kz} + C_4e^{Kz}, \\ \Pi_2(z) = C_1e^{-Kz} + C_2e^{Kz}, \\ U_1(z) = -iKk_1(C_3e^{-Kz} + C_4e^{Kz}), \\ U_2(z) = -iKk_2(C_1e^{-Kz} + C_2e^{Kz}), \\ V_1(z) = -Kk_1(C_3e^{-Kz} - C_4e^{Kz}), \\ V_2(z) = -Kk_2(C_1e^{-Kz} - C_2e^{Kz}). \end{cases} \tag{69}$$

When solution (69) is substituted into (57)–(62), we obtain a system of linear algebraic equations concerning the variables  $C_i$  ( $i = 1, \dots, 6$ ).

$$\begin{cases} C_3e^{-KH_1(t)} + C_4e^{KH_1(t)} + \frac{(k_1\rho_1 - k_2\rho_2)gH_2(t) + k_2\Delta P}{(k_1 - k_2)H_2(t) + k_2H_1(t)}C_5 = 0, \\ C_1 + C_2 = 0, \\ (e^{KH_2(t)} - e^{-KH_2(t)})C_1 + e^{-KH_2(t)}C_3 + e^{KH_2(t)}C_4 \\ + \frac{-g(k_1\rho_1 - k_2\rho_2)H_1(t) - \Delta P(k_1 - k_2)}{(k_1 - k_2)H_2(t) + k_2H_1(t)}C_6 = 0, \\ k_1(C_3e^{-KH_2(t)} - C_4e^{KH_2(t)}) - k_2(C_1e^{-KH_2(t)} - C_2e^{KH_2(t)}) = 0, \\ k_1K(C_4e^{KH_1(t)} - C_3e^{-KH_1(t)}) + \lambda(t)C_5 = 0, \\ k_2K(e^{KH_2(t)} - e^{-KH_2(t)})C_1 + \lambda(t)C_6 = 0, \end{cases} \tag{70}$$

where

$$\lambda(t) = \frac{f'(t)}{f(t)}. \tag{71}$$

The system of Equations (70) has a non-trivial solution if the determinant of the coefficient matrix is equal to zero.

Solving the resulting quadratic equation, we find:

$$\lambda_{1,2}(t) = \frac{-b \pm \sqrt{b^2 - 4ac}}{2a}, \tag{72}$$

where

$$a = 2K((k_1 + k_2) \sinh(K(L + H_2(t))) + (k_2 - k_1) \sinh(K(L - H_2(t))))), \tag{73}$$

$$b = \frac{2k_1K^2(B_1 \cosh(K(L - H_2(t))) + B_2 \cosh(K(L + H_2(t))))}{(k_1 - k_2)H_2(t) + (L + H_2(t))k_2}, \tag{74}$$

$$c = -B_3 2(\sinh(K(L - H_2(t))) + \sinh(K(L + H_2(t))))), \tag{75}$$

$$B_1 = -((k_1 - k_2)H_2(t) + (L + H_2(t))k_2)(k_1\rho_1 - k_2\rho_2)g, \tag{76}$$

$$B_2 = g(k_1 + k_2)(k_1\rho_1 - k_2\rho_2)H_2(t) - (g(k_1\rho_1 - k_2\rho_2)(L + H_2(t)) + 2k_1\Delta P)k_2, \tag{77}$$

$$B_3 = \frac{k_1^2K^3g(L + H_2(t))(k_1\rho_1 - k_2\rho_2)}{((k_1 - k_2)H_2(t) + k_2(L + H_2(t)))^2} - \frac{k_1^2K^3\Delta P(k_1 - k_2)((k_1\rho_1 - k_2\rho_2)gH_2(t) - k_2\Delta P)}{((k_1 - k_2)H_2(t) + k_2(L + H_2(t)))^2}. \tag{78}$$

Approximate expressions for  $F_{jk} = \lambda_j(t)/k_1$  at  $K \ll 1$  and  $K \gg 1$  are obtained in Appendix A.

Next, we consider the filtration flow without gravity since, as shown in [7], the presence of gravity does not affect the fundamental features of the instability development in the considered problem. We put  $g = 0$  in (72)–(78) and obtain:

$$a = 2K((k_1 + k_2) \sinh (K(L + H_2(t))) + (k_2 - k_1) \sinh (K(L - H_2(t)))) \tag{79}$$

$$b = \frac{-4k_1^2 k_2 \Delta P K^2 \cosh (K(L + H_2(t)))}{(k_1 - k_2) H_2(t) + (L + H_2(t)) k_2} \tag{80}$$

$$c = -\frac{2k_1^2 K^3 \Delta P (k_1 - k_2) k_2 \Delta P (\sinh (K(L - H_2(t))) + \sinh (K(L + H_2(t))))}{((k_1 - k_2) H_2(t) + k_2(L + H_2(t)))^2} \tag{81}$$

From the expressions (66) and (67), it follows that the ratio of coefficients  $C_6/C_5$  is equal to the ratio of perturbation amplitudes at the water–oil and water–gas boundaries. We introduce the variables  $A_{1r} = C_6/C_5$  at  $\lambda = \lambda_1$  and  $A_{2r} = C_6/C_5$  at  $\lambda = \lambda_2$ . From the system of Equations (70), we find

$$A_{1r} = \frac{-4e^{KL} \cosh (K) \sinh (KL) A + 2e^{-KL+K} \cosh (K) B}{4k_r \sinh (K) e^{KL} A + C} \tag{82}$$

$$A_{2r} = \frac{-4e^{KL} \cosh (K) \sinh (KL) A - 2e^{-KL+K} \cosh (K) B}{4k_r \sinh (K) e^{KL} A + C} \tag{83}$$

where

$$\begin{aligned} A &= ((-2k_r + 2)e^{(4L+2)K} + (2(k_r + 1)^2 - 6)e^{2K(1+L)} + (2k_r - 2)e^{2K(2+L)} + \\ &e^{4K(1+L)} + (k_r - 1)^2 e^{4KL} + (2k_r - 2)e^{2KL} + (k_r - 1)^2 e^{4K} + 1 + (-2k_r + 2)e^{2K})^{\frac{1}{2}}, \\ B &= 2 e^{3KL} (3k_r \sinh (K) - (k_r - 1) \sinh (2KL - K) + \sinh (2KL + K)), \\ C &= 2 e^{2KL+K} (2(k_r - 1)^2 \sinh (KL - 2K) + \\ &(6 - 2(k_r + 1)^2) \sinh (KL) + 2 \sinh (KL + 2K)). \end{aligned} \tag{84}$$

We consider the case when, at the initial moment, there are perturbations of the gas–water interfaces and water–oil interface in the form of

$$s_1(x, 0) = A_{0,g} \cos (Kx), \tag{85}$$

$$s_2(x, 0) = A_{0,w} \cos (Kx). \tag{86}$$

Under such initial conditions, the solution has the form

$$s_1(x, t) = (A_{1,g} e^{\lambda_1 t} + A_{2,g} e^{\lambda_2 t}) \cos (Kx), \tag{87}$$

$$s_2(x, t) = (A_{1,w} e^{\lambda_1 t} + A_{2,w} e^{\lambda_2 t}) \cos (Kx), \tag{88}$$

where the coefficients  $A_{1,g}, A_{2,g}, A_{1,w}$  and  $A_{2,w}$  are connected by the relations

$$A_{1,g} + A_{2,g} = A_{0,g}, \tag{89}$$

$$A_{1,w} + A_{2,w} = A_{0,w}, \tag{90}$$

$$A_{1,w} = A_{1r} A_{1,g}, \tag{91}$$

$$A_{2,w} = A_{2r} A_{2,g}. \tag{92}$$

From Equations (89)–(92), we find

$$A_{1,g} = -\frac{A_{0,g}A_{2r} - A_{0,w}}{A_{1r} - A_{2r}}, \tag{93}$$

$$A_{2,g} = \frac{A_{0,g}A_{1r} - A_{0,w}}{A_{1r} - A_{2r}}, \tag{94}$$

$$A_{1,w} = -\frac{A_{1r}(A_{2r}A_{0,g} - A_{0,w})}{A_{1r} - A_{2r}}, \tag{95}$$

$$A_{2,w} = \frac{A_{2r}(A_{1r}A_{0,g} - A_{0,w})}{A_{1r} - A_{2r}}. \tag{96}$$

By replacing the relations (93)–(96) in the solution of (87) and (88), we obtain

$$s_1(x, t) = \frac{-(A_{0,g}A_{2r} - A_{0,w})e^{\lambda_2 t} + (A_{0,g}A_{1r} - A_{0,w})e^{\lambda_1 t}}{A_{1r} - A_{2r}} \cos(Kx), \tag{97}$$

$$s_2(x, t) = \frac{-A_{1r}(A_{2r}A_{0,g} - A_{0,w})e^{\lambda_2 t} + A_{2r}(A_{1r}A_{0,g} - A_{0,w})e^{\lambda_1 t}}{A_{1r} - A_{2r}} \cos(Kx). \tag{98}$$

Approximate expressions for  $A_{1r}$  and  $A_{2r}$  at  $K \ll 1$  and  $K \gg 1$  are obtained in Appendix A.

The linearized equations (61) and (62) are found under the assumption that

$$\left| \frac{\partial s_1(x, t)}{\partial x} \right| \ll 1, \tag{99}$$

$$\left| \frac{\partial s_2(x, t)}{\partial x} \right| \ll 1. \tag{100}$$

Then, if the functions  $s_1(x, t)$  and  $s_2(x, t)$  are of the form (66) and (67), then the following conditions must be true

$$|KC_5 f(t)| \ll 1, \tag{101}$$

$$|KC_6 f(t)| \ll 1. \tag{102}$$

Because  $|C_5 f(t)|$  and  $|C_6 f(t)|$  are perturbation amplitudes, it follows from the above inequalities that a linear analysis is only applicable when the perturbation amplitude of the interface is much smaller than the wavelength of the perturbation.

### 5. Discussion of Results

The formation of gas or water fingers in the oil-occupied region is associated with the instability of the gas–water or water–oil boundaries. We will consider the evolution of these boundaries in two cases. In the first case, we will assume that perturbations exist only on the gas–water surface at the initial moment. In the second case, we will assume that there are perturbations on both surfaces at the initial moment, and these perturbations have equal amplitudes.

Let us put

$$H_0^* = H_2^*(0), P_0^* = P_a^* - P_L^*, V_0^* = \frac{k^*}{\mu_2^*} P_0^* / H_0^*; \tag{103}$$

then,  $k_2 = 1$  and  $k_1 = k_2 k_r$ , where the superscript \* denotes the dimensional quantities and  $k_r = k_1 / k_2$ .

According to [28], oil’s viscosity can vary from 0.0001 Pa·s to 0.8 Pa·s, while the viscosity of water is 0.001 Pa·s. Thus, the value of  $k_r$  varies from 0.1 to 800.

Substituting  $H_2(0) = 1$ ,  $H_2(t_{max}) = 0$ ,  $P_0 = \Delta P = 1$ ,  $k_2 = 1$  and  $k_1 = k_r$  into (41), we obtain that

$$t_{max} = \frac{k_r + 2L}{2k_r}, \tag{104}$$

where  $t_{max}$  is the time for oil to be completely displaced by water from the reservoir if both interfaces remain flat.

To investigate the effect of gas–water surface perturbation growth on the evolution of the water–oil surface, we consider the case when there is a perturbation of the gas–water interface at the initial moment and the water–oil interface is flat, i.e.,  $A_{0,w} = 0$ .

We denote the amplitude of the water–oil surface perturbation as  $A_w$  and the gas–water perturbation as  $A_g$ ; then, we obtain from (97) and (98) at  $A_{0,w} = 0$ :

$$A_g = \frac{A_{0,g}(A_{1r}e^{\lambda_2 t} - A_{2r}e^{\lambda_1 t})}{A_{1r} - A_{2r}}, \tag{105}$$

$$A_w = \frac{A_{0,g}A_{1r}A_{2r}(e^{\lambda_2 t} - e^{\lambda_1 t})}{A_{1r} - A_{2r}}. \tag{106}$$

The amplitude of the water–gas surface perturbation,  $A_*$ , at time  $t_* = c_t t_{max}$  is

$$A_* = \frac{A_{0,g}A_{1r}A_{2r}(e^{\lambda_2 t_*} - e^{\lambda_1 t_*})}{A_{1r} - A_{2r}}, \tag{107}$$

where  $0 < c_t < 1$ .

The value of  $A_*/A_{0,g}$  depends on the problem parameters  $c_t$ ,  $L$ ,  $k_r$  and wave number,  $K$ .

In Figure 2, the dependence of  $A_*/A_{0,g}$  on  $K$  at different values of  $L$  and  $k_r$  is presented. It is seen that at fixed values of  $k_r$  and  $c_t$ , there exists such a value of  $L_*$  that the value of  $A_*/A_{0,g}$  grows unlimitedly with increasing  $K$  at  $L < L_*$  and tends to zero at  $L > L_*$ . Note that  $L_*$  depends weakly on  $k_r$  since it changes less than twice when  $k_r$  changes by a factor of 100.

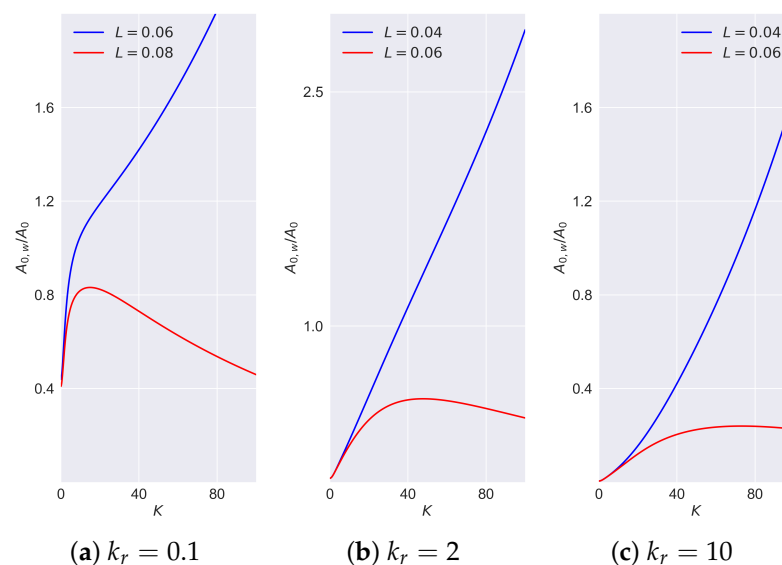


Figure 2.  $A_*/A_{0,g}$  vs.  $K$  at different water-saturated layer thicknesses,  $L$ , and  $c_t = 0.1$ .

To find approximate explicit expression for  $L_*$  at  $K \gg 1$ , we use the approximate expressions for  $\lambda_1, \lambda_2, A_{1r}$  and  $A_{2r}$  obtained in Appendix A. From

$$s_1(x, t) \sim e^{-KL} e^{\frac{Kk_r t}{L+k_r}} \cos(Kx), \tag{108}$$

at  $t = t_*$ , and taking into account the relation (104), we obtain

$$s_1(x, t_*) \sim e^{-\frac{K(2L^2+2(k_r-c_t)L-c_t k_r)}{2L+2k_r}} \cos(Kx). \tag{109}$$

It follows from the formula (109) that  $A_*/A_{0,g}$  does not increase with  $K \rightarrow \infty$  if

$$2L^2 + 2(k_r - c_t)L - c_t k_r > 0. \tag{110}$$

The inequality (110) is satisfied at

$$L > L_* = \frac{c_t - k_r + \sqrt{c_t^2 + k_r^2}}{2}. \tag{111}$$

From (111), we obtain that if  $c_t = 0.1$ , then  $L_* = 0.071$  at  $k_r = 0.1$ ,  $L_* = 0.051$  at  $k_r = 2$  and  $L_* = 0.050$  at  $k_r = 10$ . These threshold values of  $L_*$  are consistent with the results presented in Figure 2.

Thus, over time  $t_*$ , the development of short-wave perturbations at the gas–water boundary does not significantly affect the evolution of the water–oil boundary if the thickness of the water layer exceeds  $L_*$ . The velocity perturbations, which are caused by the gas–water boundary instability, decay with a decreasing  $z$  coordinate according to the law  $e^{Kz}$  in accordance with (69). At the initial moments of time, these velocity perturbations are so small at  $z = 1$  (at the water–oil surface) that during the time  $t_*$ , the amplitude  $A_w$  increases only up to a value of the order of  $A_{0,g}$ . Note that the amplitude of the perturbations of the water–gas surface at time  $t_*$  increases by more than two orders of magnitude for short-wave perturbations with wave number  $K > 100$ , as shown in Figure 3.

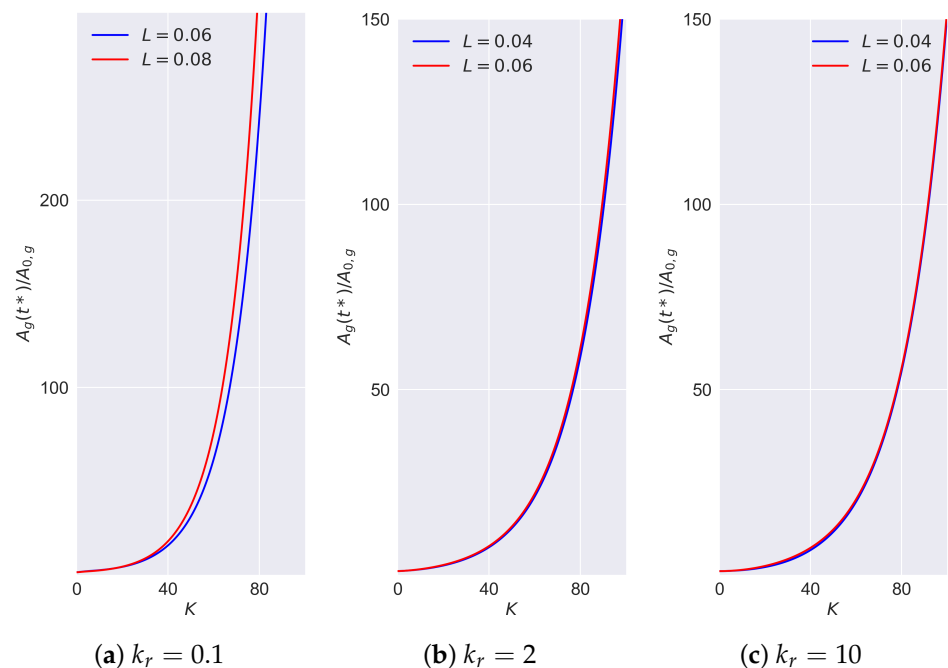


**Figure 3.**  $A_g(t_*)/A_{0,g}$  vs.  $K$  at different thicknesses of the water-bearing region layer  $L$  and  $c_t = 0.1$ .

For  $k_r > 1$ , the viscosity of water is less than that of oil, so the water–oil contact surface is unstable if oil is displaced by water. However, at  $L > L_*$ , instability development occurs

at each boundary independently. The growth of perturbations at the gas–water boundary occurs with a characteristic time of  $1/\lambda_1$ , and the growth of perturbations at the water–oil boundary occurs with a characteristic time of  $1/\lambda_2$ . Since  $\lambda_1 > \lambda_2$ , the water–oil boundary perturbations grow slower if the initial perturbation amplitude  $A_{0,w}$  is comparable to  $A_{0,g}$ .

Appendix A shows that the expressions for  $\lambda_1$  and  $\lambda_2$  at  $K \gg \max(1, L)$  can be written as

$$\lambda_1 = K \frac{k_r}{L + k_r}, \tag{112}$$

$$\lambda_2 = K \frac{k_r(k_r - 1)}{(L + k_r)(1 + k_r)}. \tag{113}$$

From the relations (112) and (113), we have

$$\frac{\lambda_2}{\lambda_1} = \frac{k_r - 1}{k_r + 1}. \tag{114}$$

If the perturbation amplitudes are equal at the initial moment, i.e.,  $A_{0,g} = A_{0,w}$ , and the perturbations develop independently, then at  $K \gg \max(1, L)$ ,

$$\frac{A_g}{A_w} \sim e^{(\lambda_1 - \lambda_2)t} = e^{\frac{2Kk_r}{(L+k_r)(k_r+1)}}. \tag{115}$$

Substituting  $t = t_*$  into the expression (115), we obtain that

$$\frac{A_g}{A_w} \sim e^{\frac{4Kk_r c_t L}{(k_r+1)(k_r+2L)}}. \tag{116}$$

Figure 4 shows the ratio of amplitudes  $A_g/A_w$  at time  $t_*$ , calculated from the Formula (116), for large values of  $K$ .

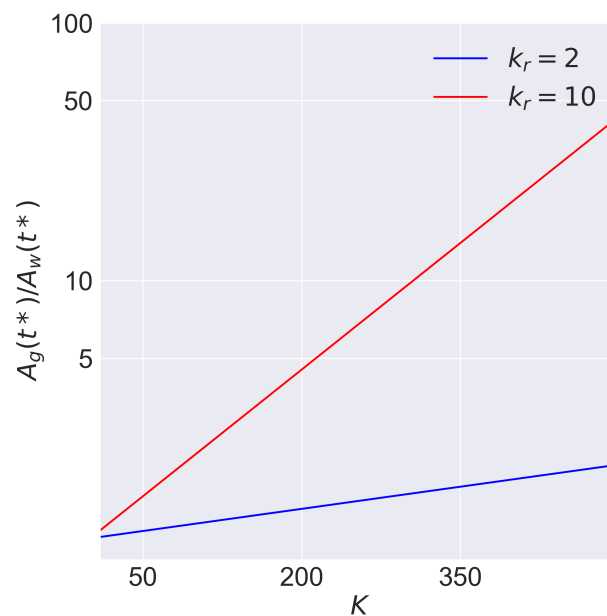


Figure 4.  $A_g/A_w$  vs.  $K$  at  $t = t_*$ ,  $c_t = 0.1$  and  $L = 0.1$ .

Figure 4 shows that in the considered case, if the initial perturbation amplitudes of both surfaces are equal, the short-wave perturbations at the water–gas boundary grow faster than at the water–oil boundary.

### 6. Conclusions

In oil field development, the displacement of oil by gas leads to the formation of gas fingers and areas with residual oil in the reservoir. If there is a layer of water between the gas and oil, gas fingers form in the area occupied by water and form areas with slow-moving water rather than oil. In most cases, oil’s viscosity is more than water’s, so the water–oil boundary is also unstable. The short-wavelength instability of this boundary leads to the formation of water fingers in the region occupied by oil. Using the normal mode method, relations describing the growth of gas–water and water–oil surface perturbations are obtained. These relations describe the evolution of perturbations in the linear approximation, depending on the wavelength of the perturbation and the parameters of the main flow. The study shows that there is a threshold value of water layer thickness,  $L_*$ . Suppose the thickness of the water layer is greater than the threshold value. In that case, the development of perturbations at the water–gas boundary has no effect on the development of perturbations for a time comparable to the characteristic time of the oil displacement process. An expression for calculating the threshold value of  $L_*$  at given values of oil viscosity, pressure drop and thickness of the low-permeable layer of porous medium containing oil is obtained. It is shown that short-wave perturbations at the water–oil boundary grow much slower than perturbations at the water–gas boundary at the linear stage of perturbation evolution.

It follows from the results that the presence of a water layer between oil and gas significantly reduces the growth of short-wave perturbations (“fingers”) in the oil-occupied region. Thus, the water layer may allow the amount of residual oil to be reduced, which is a big problem for effective production.

The study was performed for small perturbations under the assumption that the wavelength of the perturbation remains much larger than the amplitude. The evolution of perturbations at the nonlinear stage is planned to be investigated in the future using the continuum and network models previously described by the authors in [9].

**Author Contributions:** Conceptualization, V.S. and G.T.; funding acquisition, G.T.; investigation, V.S. and P.K.; methodology, V.S. and G.T.; project administration, G.T.; resources, V.S.; software, P.K.; supervision, V.S.; validation, P.K.; visualization, P.K.; writing—original draft, P.K.; writing—review and editing, V.S. and G.T. All authors have read and agreed to the published version of the manuscript.

**Funding:** The work was carried out with support from the Russian Science Foundation under grant no. 21-11-00126.

**Institutional Review Board Statement:** Not applicable.

**Informed Consent Statement:** Not applicable.

**Data Availability Statement:** Not applicable.

**Acknowledgments:** The authors wish to express their very sincere thanks to the reviewers for their valuable comments and suggestions on this work.

**Conflicts of Interest:** The authors declare no conflict of interest.

### Appendix A

From the solution (72) at  $K \ll 1$ , i.e., long waves, we obtain an approximate expression for  $F_{jk}$  ( $j$  being the solution number):

$$F_{1k} = \frac{k_r^2}{(L + k_r)^2} + \frac{(k_r^3 + (L^3 - 3L^2 + 3L)k_r^2 + 3k_r(2L^2 - L^3) + 3L^3)K^2}{3(L + k_r)^3}, \tag{A1}$$

$$F_{2k} = \frac{L(k_r - 1)}{L + k_r} K^2, \tag{A2}$$

where  $k_r = k_1/k_2$ .

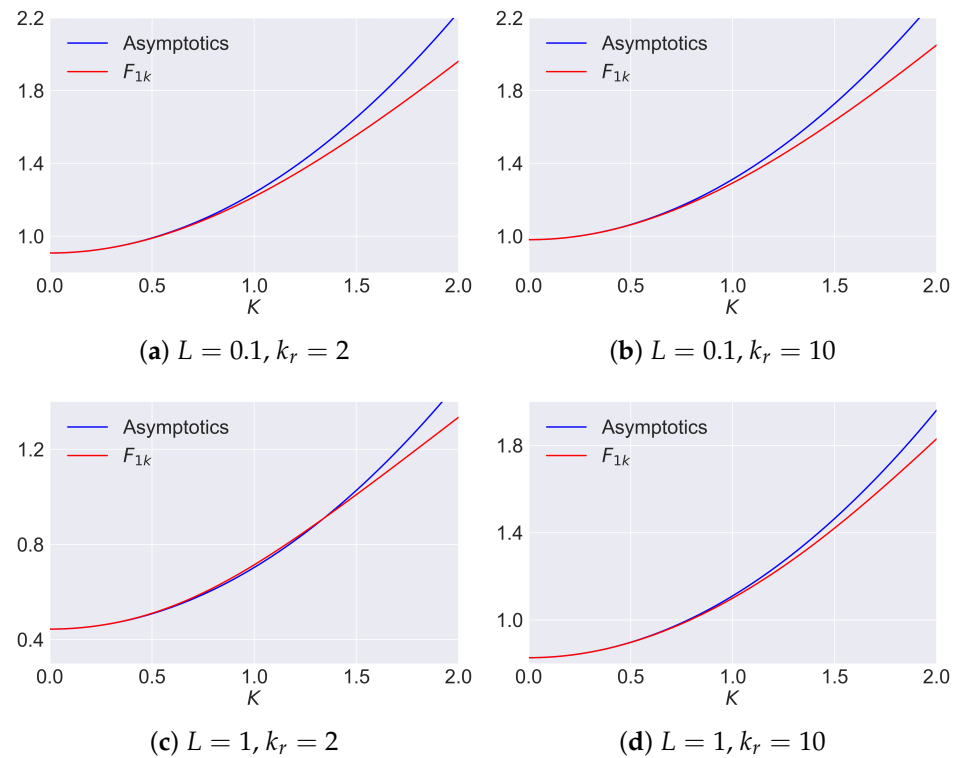


**Figure A1.** Convergence of the obtained asymptotics of the function  $F_{1k}$  at small  $K \ll 1$ .

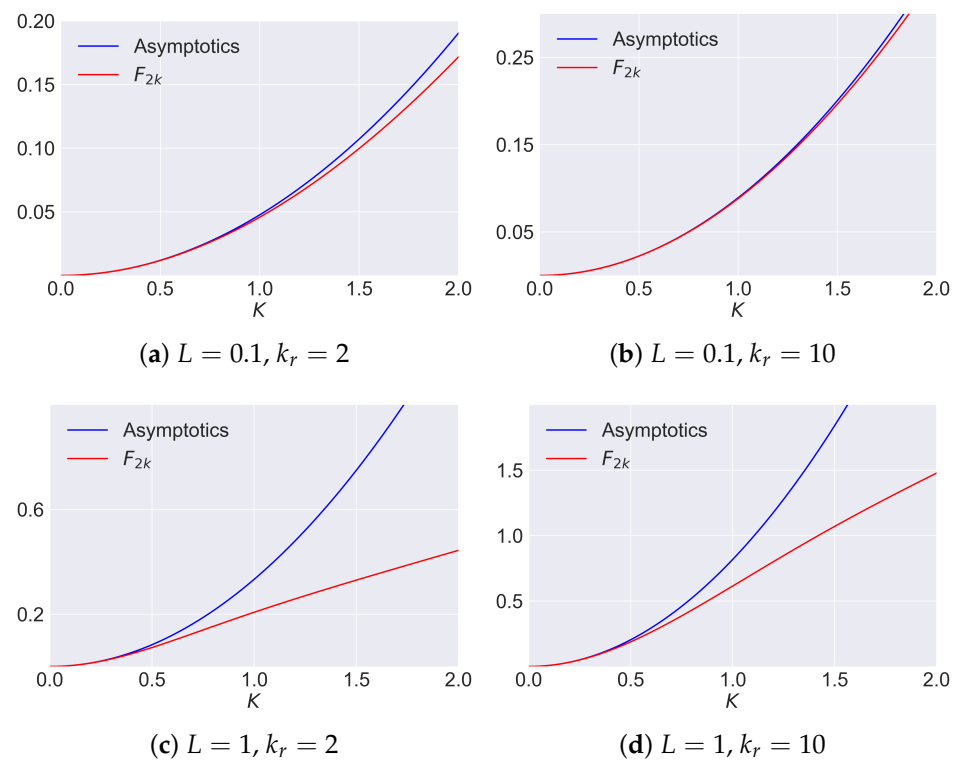


**Figure A2.** Convergence of the obtained asymptotics of the function  $F_{2k}$  at small  $K$ .

Figure A1a–d shows that if  $L < 1$ , the expression (A1) approximates (72) well at  $K < 0.5$ . There is also agreement between the results obtained by the relation (72) and the approximate formula (A2) (see Figure A2).



For short-wave perturbations at  $K \gg 1$ , from the relation (72), we find

$$F_{1k} = K \frac{k_r}{L + k_r}, \tag{A3}$$

$$F_{2k} = K \frac{k_r(k_r - 1)}{(L + k_r)(1 + k_r)}. \tag{A4}$$

Figures A3a,b and A4a,b show that for short-wave perturbations, the approximate relations (A3) and (A4) allow us to perform the calculations with good accuracy at  $K > 20$ .

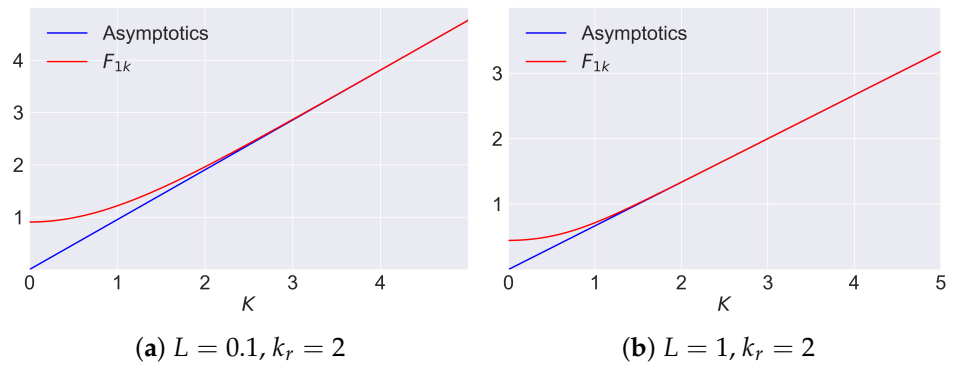


Figure A3. Verification of approximation of the function  $F_{1k}$  at large  $K$ .

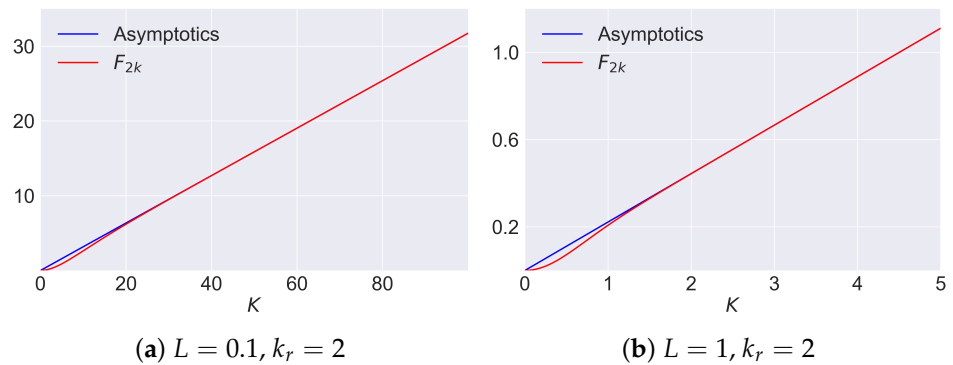


Figure A4. Verification of approximation of the function  $F_{2k}$  at large  $K$ .

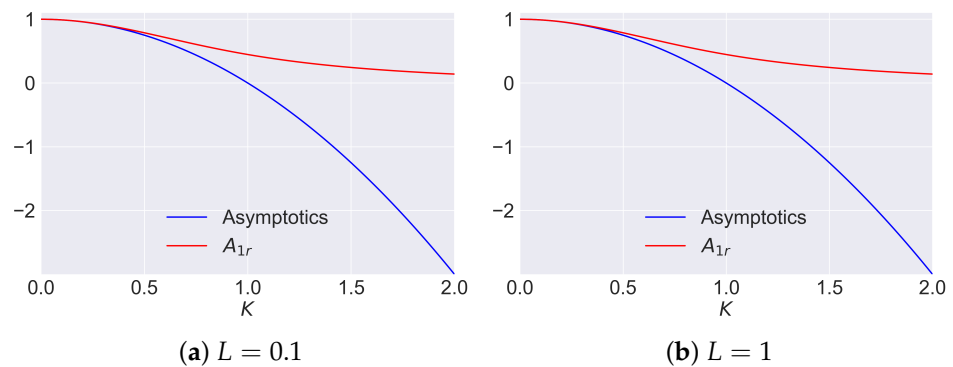


Figure A5. Comparison of approximate and precise solution for small  $K$  for  $A_{1r}$ .

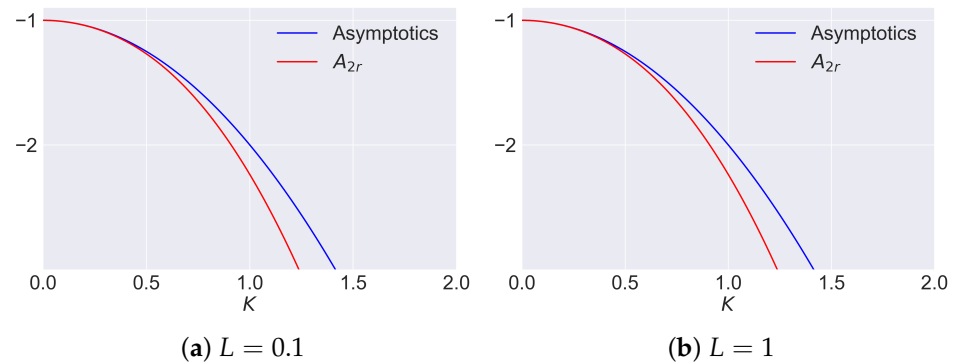


Figure A6. Comparison of approximate and precise solution for small  $K$  for  $A_{2r}$ .

The relation (82) at  $K \ll 1$  can be replaced by the approximate expression

$$A_{1r} = 1 - \frac{((2 - L)k_r + 2L)LK^2}{2k_r}, \tag{A5}$$

and at  $K \gg 1$ , by the expression

$$A_{1r} = e^{-KL}. \tag{A6}$$

For the second solution, in the same notations, the relation is as follows:

$$A_{2r} = \frac{-4e^{KL} \cosh(K) \sinh(KL)A - 2e^{-KL+K} \cosh(K)B}{4k_r \sinh(K)e^{KL}A + C}, \tag{A7}$$

which at  $K \ll 1$  can be replaced by

$$A_{2r} = -\frac{1}{k_r - 1} \left( 1 + \frac{((2 - L)k_r + 2L)LK^2}{2k_r} \right), \tag{A8}$$

and for short-wave perturbations

$$A_{2r} = -e^{KL}. \tag{A9}$$

Figures A5a,b and A6a,b illustrate the applicability of the expressions (A5)–(A9) for small values of the wave number,  $K$ . A comparison of the exact and approximate expressions obtained for large  $K$  is performed in Figures A7a,b and A8a,b.

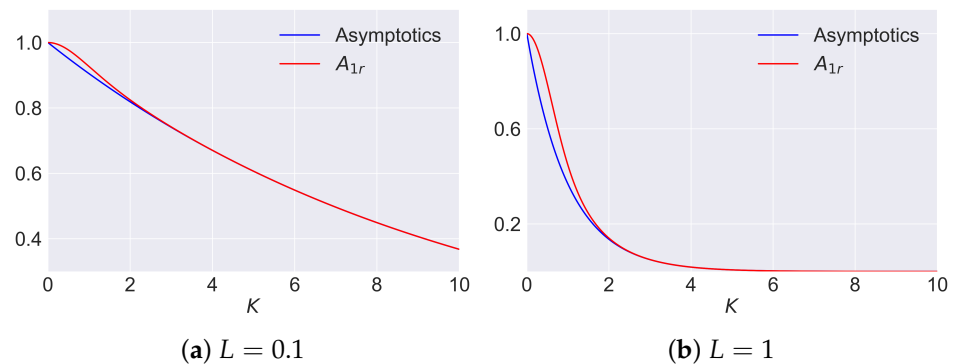


Figure A7. Comparison of approximate and precise solution for large  $K$  for  $A_{1r}$ .

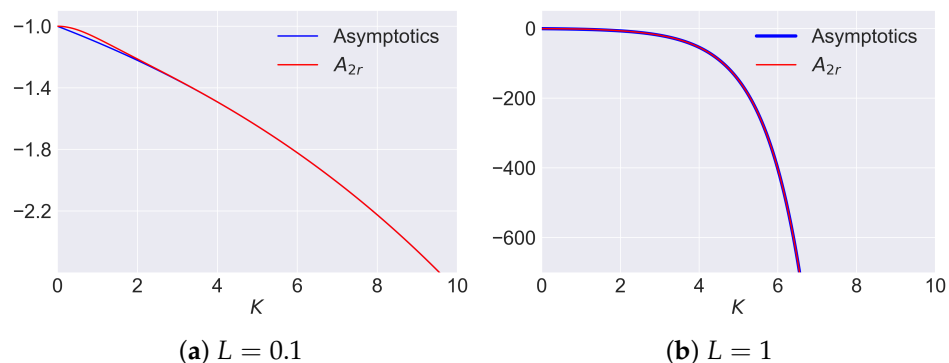


Figure A8. Comparison of approximate and precise solution for large  $K$  for  $A_{2r}$ .

## References

- Lapuk, B. *Theoretical Foundations for the Development of Natural Gas Fields*; Institute for Computer Research: Moscow-Izhevsk, Russia, 2002.
- Rostami, B.; Kharrat, R.; Ghotbi, C.; Tabatabaie, S. Gas-Oil relative Permeability and Residual Oil Saturation as Related to Displacement Instability and Dimensionless Numbers. *Oil Gas Sci. Technol.* **2010**, *65*, 299–313. [\[CrossRef\]](#)
- Kim, V.; Kim, S.; Chung, B.J.; Choi, C. Convective instability in a horizontal porous layer saturated with oil and a layer of gas underlying it. *Int. J. Heat Mass Transf.* **2003**, *30*, 225–234. [\[CrossRef\]](#)
- Tsyppkin, G.; Shargatov, V. Influence of capillary pressure gradient on connectivity of flow through a porous medium. *Int. J. Heat Mass Transf.* **2018**, *127*, 1053–1063. [\[CrossRef\]](#)
- Rao, D.; Ayirala, S.; Kulkarni, M.; Sharma, A. Development of Gas Assisted Gravity Drainage (GAGD) Process for Improved Light Oil Recovery. In Proceedings of the SPE/DOE Symposium on Improved Oil Recovery, Tulsa, Oklahoma, 13–17 April 2004. [\[CrossRef\]](#)
- Zhu, X.; Chen, L.; Wang, S.; Feng, Q.; Tao, W. Pore-scale study of three-phase displacement in porous media. *Phys. Fluids* **2022**, *34*, 043320.
- Shargatov, V.; Il'ichev, A.; Tsyppkin, G. Dynamics and stability of moving fronts of water evaporation in a porous medium. *Int. J. Heat Mass Transf.* **2015**, *83*, 552–561. [\[CrossRef\]](#)
- Saffman, P.G.; Taylor, G. The penetration of a fluid into a porous medium or Hele-Shaw cell containing a more viscous liquid. *Proc. R. Soc. Lond. Ser. A Math. Phys. Sci.* **1958**, *245*, 312–329. [\[CrossRef\]](#)
- Shargatov, V.; Tsyppkin, G.G.; Gorkunov, S.V.; Kozhurina, P.I.; Bogdanova, Y.A. On the Short Wave Instability of the Liquid/Gas Contact Surface in Porous Media. *Mathematics* **2022**, *10*, 3177. [\[CrossRef\]](#)
- Tsyppkin, G.; Shargatov, V. Linear stability of a filtration flow with gas-oil interface within the brinkman approach. *Fluid Dyn.* **2022**, *57*, 273–280. [\[CrossRef\]](#)
- Alizadeh, A.; Piri, M. Three-phase flow in porous media: A review of experimental studies on relative permeability. *Rev. Geophys.* **2014**, *52*, 468–521.
- Arshadi, M.; Khishvand, M.; Aghaei, A.; Piri, M.; Al-Muntasheri, G. Pore-Scale Experimental Investigation of Two-Phase Flow Through Fractured Porous Media. *Water Resour. Res.* **2018**, *54*, 3602–3631.
- Khan, Z.; Pritchard, D. Liquid–vapour fronts in porous media: Multiplicity and stability of front positions. *Int. J. Heat Mass Transf.* **2013**, *61*, 1–17. [\[CrossRef\]](#)
- Khan, Z.; Pritchard, D. Anomaly of spontaneous transition to instability of liquid–vapour front in a porous medium. *Int. J. Heat Mass Transf.* **2015**, *84*, 448–455. [\[CrossRef\]](#)
- Balashova, G. Movement of two fluids in a layered porous formation. *Tavrisheskij Vestn. Inform. I Mat.* **2018**, *4*, 57–66.
- Latham, K.; Latham, J.P.; Pavlidis, D.; Xiang, J.; Fang, F.; Mostaghimi, P.; Percival, J.; Pain, C.; Jackson, M. Multiphase flow simulation through porous media with explicitly resolved fractures. *Geofluids* **2015**, *15*, 592–607. [\[CrossRef\]](#)
- Bublik, S.; Semin, M. Numerical Simulation of the Filtration of a Steam–Water–Oil Mixture during the Thermal-Steam Treatment of a Reservoir. *Math. Model. Comput. Simulations* **2022**, *14*, 335–348. [\[CrossRef\]](#)
- Bublik, S.; Semin, M. Numerical Simulation of Phase Transitions in Porous Media with Three-Phase Flows Considering Steam Injection into the Oil Reservoir. *Computation* **2022**, *10*, 205. [\[CrossRef\]](#)
- Wagner, Q.; Adolfo, P.; Alvaro, M. Analytical solution for one-dimensional three-phase incompressible flow in porous media for concave relative permeability curves. *Int. J. Non-Linear Mech.* **2021**, *137*, 103792. [\[CrossRef\]](#)
- Das, M.; Mukherjee, P.; Muralidhar, K. *Modeling Transport Phenomena in Porous Media with Applications*; Springer International Publishing: Berlin/Heidelberg, Germany, 2018. [\[CrossRef\]](#)
- Kalaydjian, F.J.M.; Moulu, J.C.; Vizika, O.; Munkerud, P.K. Three-phase flow in water-wet porous media: Gas/oil relative permeabilities for various spreading conditions. *J. Pet. Sci. Eng.* **1997**, *17*, 275–290. [\[CrossRef\]](#)

22. Pereira, G.; Pinczewski, W.; Chan, D.; Paterson, L.; Øren, P. Pore-scale network model for drainage-dominated three-phase flow in porous media. *Transp. Porous Media* **1996**, *24*, 167–201. [[CrossRef](#)]
23. van Dijke, M.; Sorbie, K.; Sohrabi, M.; Danesh, A. Three-Phase Flow WAG Processes in Mixed-Wet Porous Media: Pore-Scale Network Simulations and Comparison with Water-Wet Micromodel Experiments. *SPE J.* **2004**, *9*, 57–66.
24. Ying, J.; Zhao, H.; Wang, Z.; An, K.; Cao, Q.; Li, C.; Jia, J.; Zhang, Z.; Liu, X. Effect of asphaltene structure characteristics on asphaltene accumulation at oil-water interface: An MD simulation study. *Colloids Surfaces A Physicochem. Eng. Asp.* **2023**, *675*, 132014. [[CrossRef](#)]
25. Tirjoo, A.; Bayati, B.; Rezaei, H.; Rahmati, M. Molecular dynamics simulation of the effect of ions in water on the asphaltene aggregation. *J. Mol. Liq.* **2019**, *277*, 40–48. [[CrossRef](#)]
26. Khormali, A. Effect of water cut on the performance of an asphaltene inhibitor package: Experimental and modeling analysis. *Pet. Sci. Technol.* **2022**, *40*, 2890–2906. [[CrossRef](#)]
27. Schubert, G.; Straus, J. Gravitational stability of water over steam in vapor-dominated geothermal systems. *J. Geophys. Res. Solid Earth* **1980**, *85*, 6505–6512. [[CrossRef](#)]
28. Trebin, G.; Charygin, N.; Obuhova, T. *Oil Fields of the Soviet Union*; Nedra: Moscow, Russia, 1980.

**Disclaimer/Publisher’s Note:** The statements, opinions and data contained in all publications are solely those of the individual author(s) and contributor(s) and not of MDPI and/or the editor(s). MDPI and/or the editor(s) disclaim responsibility for any injury to people or property resulting from any ideas, methods, instructions or products referred to in the content.